Journal of Photoscience (2000), Vol. 7(4), pp. 155 – 159

DYNAMICS OF $tRNA^{val}$ MEASURED WITH A LONG-LIFETIME METAL-LIGAND COMPLEX

Jung Sook Kang*
Department of Oral Biochemistry and Molecular Biology, College of Dentistry and Research Institute for Oral Biotechnology, Pusan National University, Pusan 602-739, Korea

$[Ru(bpy)_2(dppz)]^{2+}$ (bpy = 2,2′-bipyridine, dppz = dipyrido[3,2-a:2′,3′-c]phenazine) (RuBD), a long-lifetime metal-ligand complex displays favorable photophysical properties including long lifetime, polarized emission, and very little background fluorescence. To further show the usefulness of this luminophore (RuBD) for probing nucleic acid dynamics, its intensity and anisotropy decays when bound to $tRNA^{val}$ were examined using frequency-domain fluorometry with a blue light-emitting diode (LED) as the modulated light source. Unexpectedly much longer mean lifetime was obtained at 4℃ ($<\tau>$ = 178.3 ns) as compared to at 25℃ ($<\tau>$ = 117.0 ns), suggesting more favorable conformation of $tRNA^{val}$ for RuBD when intercalated at 4℃. The anisotropy decay data showed longer rotational correlation times at 4℃ (52.7 and 13.0 ns) than at 25℃ (32.9 and 10.3 ns). The presence of two rotational correlation times suggests that RuBD reveals both local and overall rotational motion of $tRNA^{val}$. Due to long lifetime of RuBD and small size of $tRNA^{val}$, very low steady-state anisotropy values were observed, 0.048 and 0.036 at 4 and 25℃, respectively. However, a clear difference in the modulated anisotropy values was seen between 4 and 25℃. These results indicate that RuBD can be useful for studying hydrodynamics of small nucleic acids such as $tRNA^{val}$.

key words: $tRNA^{val}$; long-lifetime metal ligand complex; frequency-domain fluorometry; anisotropy decay; light-emitting diode

INTRODUCTION

Long-lifetime metal-ligand complexes (MLCs) which display decay times ranging from 100 ns to more than 10 μs have only recently become available [1-3] and have been proven to have favorable chemical, photochemical and photophysical properties. Because of large Stokes' shift, the MLCs do not self-quench [2,3]. In addition, the MLCs show good water solubility and high chemical and photochemical stability [2,3]. The long lifetimes of the MLCs allow the use of gated detection, which can be employed to suppress interfering autofluorescence from biological samples and can thus provide increased sensitivity [4]. And finally, the MLCs display polarized emission, making them useful for microsecond dynamics [2,3].

Barton and coworkers [5-7] reported that the dipyrido[3,2-a:2′,3′-c]phenazine (dppz) complexes of ruthenium appear to be a prime candidate for a spectroscopic probe for nucleic acids because of their "molecular light switch" properties for DNA. They are known to be nonfluorescent in water but emit when the dppz ligand is intercalated into the DNA helix. Emission from the dppz complexes is quenched when the nitrogens on the dppz are exposed to water. These nitrogens are shielded from water when the dppz intercalates into double-helical DNA, and the complex becomes fluorescent. Since the luminescent enhancement upon DNA binding is $\geq 10^4$, there is essentially no background with the dppz complexes of ruthenium. Lakowicz and colleagues [8,9] introduced the use of the dppz complexes of ruthenium to study the hydrodynamics of nucleic acids. Using the ruthenium complexes, they examined the intensity and anisotropy decays of calf thymus DNA and could observe rotational correlation times up to several hundred nanoseconds.

In the present study, I have examined the intensity and anisotropy decays of $[Ru(bpy)_2(dppz)]^{2+}$ (bpy = 2,2′-bipyridine) (RuBD) when bound to $tRNA^{val}$ in order to further show the usefulness of this luminophore (RuBD) for probing nucleic acid dynamics. For this study, frequency-domain fluorometry was used with a high-intensity, blue light-emitting diode (LED) as the light source. With this LED I was able to directly modulate the excitation light up to 100 MHz without the need for an external modulator like a Pockels cell which reduces the light amount to a great extent. Due to very low quantum yield (Q = 0.008) of RuBD [10], time-domain fluorometry was used in the previous studies of intensity and anisotropy decays of RuBD [8,9]. However, with a high-intensity, blue LED as the light source, I have been able to obtain very reliable time-resolved intensity and anisotropy decays using the frequency-domain method.

*To whom correspondence should be addressed.
E-mail : jsokang@hyowon.pusan.ac.kr
Received 15 November 2000; accepted 15 December 2000

MATERIALS AND METHODS

Materials $tRNA^{val}$ was obtained from Sigma (St. Louis, MO, U.S.A.) and used without further purification. RuBD was synthesized by the method described previously [8,9]. All other chemicals were of the reagent grade, and water was deionized with a Milli-Q system. All measurements were carried out in 100 mM KCl, 10 mM Tris, pH 7.4.

Absorption and steady-state fluorescence measurement The $tRNA^{val}$ concentration was 600 μM while that of RuBD was 15 M. The concentrations of $tRNA^{val}$ and RuBD were determined using molar extinction coefficients of 8,200 $M^{-1}cm^{-1}$ (expressed as nucleotide) at 260 nm and 13,000 $M^{-1}cm^{-1}$ at 440 nm, respectively. UV-visible absorption spectra were measured with a Hewlett-Packard 8453 diode array spectrophotometer. Steady-state intensity and anisotropy measurements were carried out using an Aminco SLM AB2 spectrofluorometer (Spectronic Instruments, Inc., Rochester, NY, U.S.A.). RuBD was excited at 440 nm.

Frequency-domain intensity and anisotropy decay measurements Measurements were performed using the instruments described previously [11] and modified with a data acquisition card from ISS, Inc. (Urbana, IL, U.S.A.) [12]. The excitation source was a blue LED LNG992CFBW (Panasonic, Japan) with luminous intensity of 1,500 mcd. An LED driver LDX-3412 (ILX Lightwave, Boseman, MO, U.S.A.) provided 30 mA of current at frequencies from 0.4 to 15 MHz. A 450±20 nm interference filter and a 620 nm cut-off filter were used for isolating excitation and emission, respectively. Rhodamine B in water (τ = 1.68 ns) was utilized as a lifetime standard.

The intensity decays were recovered from the frequency-domain data in terms of a multiexponential model:

$$I(t) = \sum_{i=1}^{n} \alpha_i e^{-t/\tau_i} \tag{1}$$

where the preexponential factors α_i are the amplitude of each component, $\Sigma\alpha_i = 1.0$, τ_i are the decay times, and n are the numbers of exponential components. These values were determined by nonlinear least squares analysis as described previously [13,14]. Mean lifetimes were calculated according to Eq. (2):

$$<\tau> = \frac{\sum_i \alpha_i \tau_i^2}{\sum_i \alpha_i \tau_i} = \sum_i f_i \tau_i \tag{2}$$

where f_i is the fractional steady-state contribution of each component to the total emission, and Σf_i is normalized to unity. f_i is given by

$$f_i = \frac{\alpha_i \tau_i}{\sum_j \alpha_j \tau_j} \tag{3}$$

The best fits were obtained by a minimum value for the goodness-of-fit parameters χ_R^2:

$$\chi_R^2 = \frac{1}{\nu}\sum_{\omega}\left[\left(\frac{\varphi_\omega - \varphi_{c\omega}}{\delta\varphi}\right)^2 + \left(\frac{m_\omega - m_{c\omega}}{\delta m}\right)^2\right] \tag{4}$$

where ν is the number of degrees of freedom, and φ_ω and m_ω are the experimental phase and modulation, respectively. The subscript c is used to indicate calculated values for assumed values of α_i and τ_i, and $\delta\varphi$ and δm are the experimental uncertainties. Here, the values of $\delta\varphi$ and δm were set at 0.2° and 0.005, respectively.

The frequency-domain anisotropy decays were also analyzed in terms of the multiexponential model:

$$r(t) = r_0 \sum_i g_i e^{-t/\theta_i} \tag{5}$$

where g_i is the amplitude of the anisotropy component with a rotational correlation time θ_i, $\Sigma g_i = 1.0$, and r_0 is the anisotropy in the absence of rotational diffusion. The total anisotropy r_0 was a fitted parameter.

RESULTS AND DISCUSSION

In this report, I have studied the hydrodynamic properties of $tRNA^{val}$ using a long-lifetime MLC, RuBD. The chemical structure of RuBD is shown in Fig. 1. Fig. 2 shows the emission spectrum of RuBD bound to $tRNA^{val}$, which shows an emission peak at about 620 nm. In aqueous solution the luminescence of this probe is undetectable. The frequency-domain intensity decays of RuBD bound to $tRNA^{val}$ are shown in Fig. 3. The intensity decays were best fit by a triple exponential decay. Table 1 shows the intensity decay results at 4 and 25°C. Mean lifetime values (<τ>) obtained at 4 and 25°C were 178.3 and 117.0 ns, respectively. As expected, increased decay time was observed at 4°C (about 150%) in comparison to 25°C, probably due to the reduced collisional motions at the lower temperature. However, the important point is the magnitude of the difference. I also have mea-

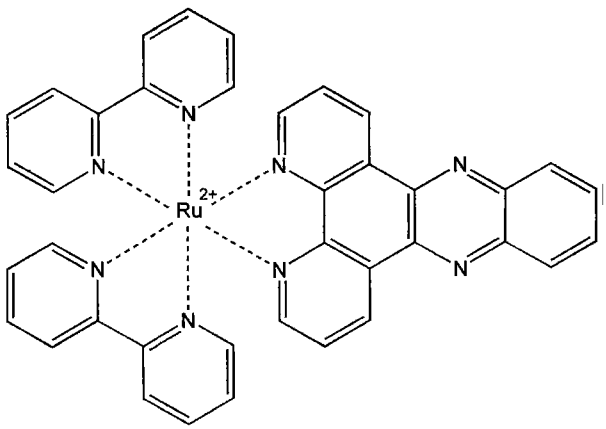

Fig. 1. Chemical structure of $[Ru(bpy)_2(dppz)]^{2+}$ (RuBD).

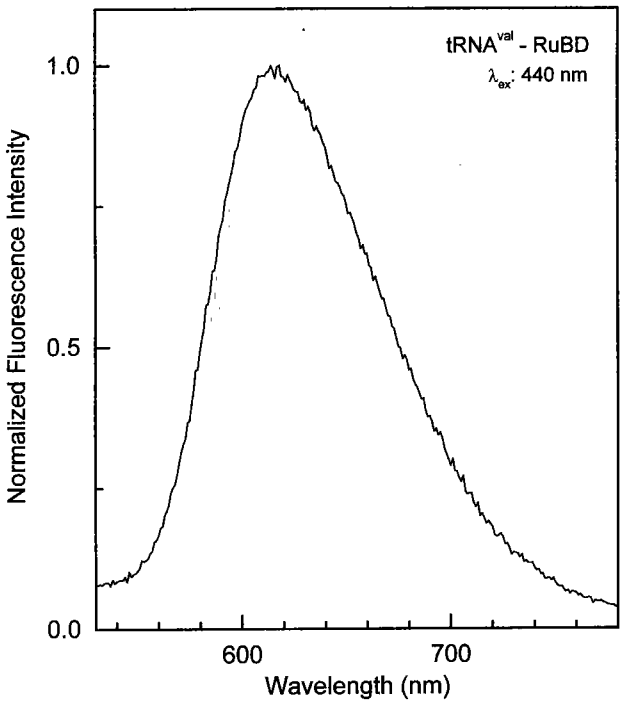

Fig. 2. Emission spectrum of $[Ru(bpy)_2(dppz)]^{2+}$ (RuBD) bound to tRNA^{val}. Excitation was at 440 nm.

Table 1. Multiexponential intensity decay analyses of $[Ru(bpy)_2(dppz)]^{2+}$ bound to tRNA^{val} at different temperatures

Temperature(°C)	τi (ns)	α_i	f_i^a	<τ>^{a} (ns)	χ_R^{2b}
4	280.3	0.12	0.55	178.3	2.5
	61.0	0.37	0.37		
	8.9	0.51	0.08		
25	180.0	0.16	0.55	117.0	2.9
	48.1	0.40	0.35		
	12.0	0.44	0.10		

[a]Fractional intensities f_i and mean lifetimes <τ> were calculated using Eqs. (3) and (2), respectively.

[b]The goodness-of-fit paramaeters χ_R^2 were calculated by Eq. (4), and the standard errors of phase angle and modulation were set at 0.2° and 0.005, respectively.

sured the intensity decays of RuBD bound to supercoiled, cut and relaxed pTZ18U plasmids at 4 and 25°C (unpublished data). However, in all forms of pTZ18U plasmids, the differences were much smaller than in tRNA^{val}. The mean intensity decay times of RuBD bound to supercoiled, cut and relaxed pTZ18U plasmids at 4°C were each about 120% of those at 25°C. It seems likely that the RuBD MLC was much more efficiently shielded from water at 4°C than at 25°C for tRNA^{val}. In other words, RuBD binds much more efficiently to tRNA^{val} at 4°C, resulting in much longer lifetime. It seems that tRNA^{val} adopts more favorable conformations for RuBD when bound at 4°C. Still, the mean lifetime at 25°C (<τ> = 117.0 ns) is comparable to the values previously reported for calf thymus DNA [6-10].

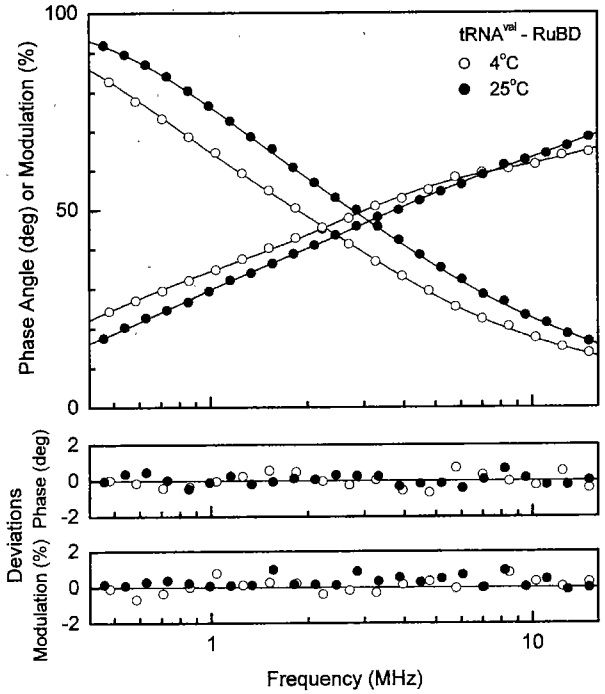

Fig. 3. Frequency-domain intensity decays of $[Ru(bpy)_2(dppz)]^{2+}$ (RuBD) bound to tRNA^{val} at 4 and 25°C. The open and closed circles represent the values at 4 and 25°C, respectively. The solid lines in the upper panel show the best triple-exponential fits to the data. The middle and lower panels show the plots of residuals between the experimental data and the fitted curves.

Table 2. Anisotropy decay analyses of $[Ru(bpy)_2(dppz)]^{2+}$ bound to tRNA^{val} at different temperatures.

Temperature(°C)	θ_i (ns)	$r_o{*}g_i$	$\Sigma(r_o{*}g_i)$	χ_R^{2a}
4	52.7	0.087	0.129	4.5
	13.0	0.042		
25	32.9	0.050	0.128	4.2
	10.3	0.078		

[a]The goodness-of-fit parameters χ_R^2 were calculated by Eq. (4), and the standard errors of phase angle and modulation were set at 0.2° and 0.005, respectively.

In addition to the intensity decay measurements, the anisotropy decays of RuBD bound to tRNA^{val} were also measured at 4 and 25°C (Fig. 4), and the results are summarized in Table 2. The best fits of the anisotropy decay data were obtained using the two exponential model. The slow rotational correlation times (52.7 and 32.9 ns at 4 and 25°C, respectively) appear to be consistent with those expected for overall rotational mobility of tRNA^{val}. The fast rotational correlation times (13.0 and 10.3 ns, respectively, at 4 and 25°C) may be due to independent motion of two helical arms of the L-shaped structure of tRNA^{val} because the correlation time constant of local internal motion of the bases within tRNA is usually in the range of picoseconds [15]. X-ray crystal struc-

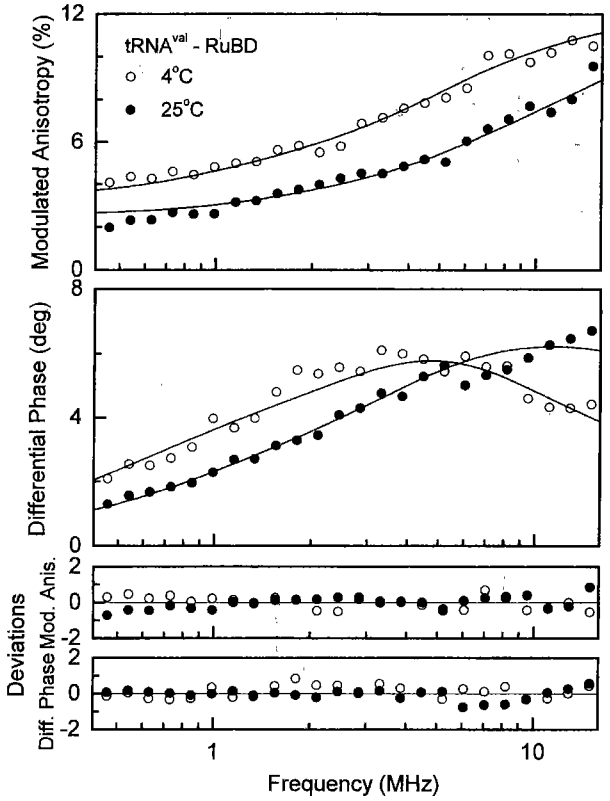

Fig. 4. Frequency-domain anisotropy decays of $[Ru(bpy)_2(dppz)]^{2+}$ (RuBD) bound to tRNA^{val} at 4 and 25℃. The open and closed circles represent the values at 4 and 25℃, respectively. The modulated anisotropies and differential phases are shown in the first and second panels, respectively. The solid lines in the first and second panels show the best double-exponential fits to the data. The lower two panels show the plots of residuals between the experimental data and the fitted curves.

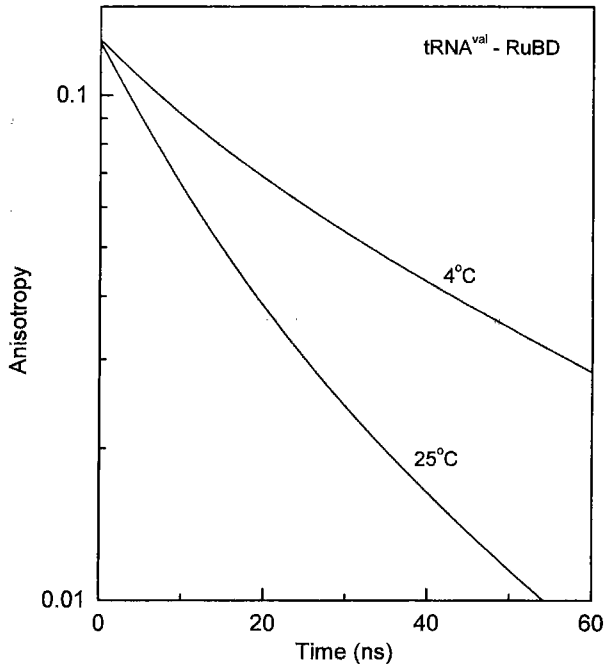

Fig. 5. Time-domain representation of anisotropy decays of $[Ru(bpy)_2(dppz)]^{2+}$ (RuBD) bound to tRNA^{val} at 4 and 25℃.

ture analyses have revealed that tRNAs have more or less the same L-shaped configuration [16,17]. From the result of the present study, it seems that the two helical arms of the L-shape show identical rotational correlation times (13.0 and 10.3 ns, respectively, at 4 and 25℃). As expected, longer rotational correlation times were observed at 4℃ (52.7 and 13.0 ns) in contrast to 25℃ (32.9 and 10.3 ns). Thus, it seems that both the overall and local rotational mobility of tRNA^{val} depend on temperature. However, it should be pointed out that the overall rotational correlation times were slightly longer than the values reported previously for tRNA^{val} by fluorescence anisotropy decays [18] and by electrooptical measurements [19]. Hence, the possibility of the presence of somewhat denatured extended form of tRNA^{val} cannot be ruled out. A plausible explanation may be the probe concentration, about 2:1 of RuBD to tRNA^{val} molar ratio. Because of very low quantum yield (Q = 0.008) of RuBD [10], quite high probe concentration was used. The absence of Mg^{2+} in the buffer, which plays an important role in tRNA conformation, can be a factor of the possibility as well. Fig. 4 (first panel) also shows the modulated anisotropy values for RuBD bound to tRNA^{val}. Of course, lower modulated anisotropy values were observed at 4℃ than those at 25℃. I also measured the steady-state anisotropy, however, the steady-state anisotropy values were quite low, 0.048 and 0.036 at 4 and 25℃, respectively. It is thus likely that RuBD, a long-lifetime MLC, is not suitable for measuring the steady-state anisotropy values of small nucleic acids. However, the results of time-resolved anisotropy decay measurements clearly showed that RuBD can be useful for studying hydrodynamics of smaller nucleic acids such as tRNA^{val}. It is informative to examine the anisotropy decays in the time-domain reconstructed from the frequency-domain data (Fig. 5). The time-domain representation of multiexponential analysis data explicitly shows an initial rapid decrease in anisotropy, followed by a slower loss of the remaining anisotropy at longer times, which is attributed to overall rotational motion of tRNA^{val}.

The dppz complexes of ruthenium bind to double helical DNA through intercalation with affinities exceeding 10^7 M^{-1}. There are two common dppz complexes of ruthenium, the bpy derivative RuBD and the 1,10-phenanthroline (phen) derivative $[Ru(phen)_2(dppz)]^{2+}$. The phen derivative has some advantages over the other bpy derivative RuBD because of its longer lifetimes and higher quantum yield [6,7,9]. However, Jenkins *et al.* [6] showed that RuBD exhibited better sensitivity to conformational differences in DNA because of the incomplete shielding of the dppz ligand from water in the presence of bpy in contrast to the other phen derivative. The use of MLCs to measure nucleic acid hydrodynamics

is just beginning, and additional MLCs for nucleic acid dynamics are yet to be developed.

An interesting aspect of this study was the use of a blue LED as the source of excitation. Using it I was able to obtain approximately 3 to 5 mW of excitation power depending on the LED current. The use of LED allowed a simpler "turn-key" operation, i.e., less optical adjustments and easier electronic operations. Direct electronic modulation of up to 100 MHz eliminates the expensive and cumbersome electro-optic modulators found in most frequency-domain instruments [20]. The low cost of LEDs, about $2 to $10 a piece, together with its simpler mode of operation will allow laboratories to perform time-resolved fluorescence measurements with less sophisticated fluorescence equipments in an economical way. In general, the use of the new high-intensity UV, blue and green GaN LEDs will facilitate the use of time-resolved measurements for many laboratories and a wide variety of applications.

Acknowledgement – I deeply thank Professor Joseph R. Lakowicz (Center for Fluorescence Spectroscopy, Dept. of Biochemistry and Molecular Biology, University of Maryland at Baltimore, Baltimore, MD, USA) for providing instrumentation and the software CFSSHELL. I am also grateful to Dr. Omoefe O. Abugo for helping the time-resolved fluorescence measurements.

REFERENCES

1. DeGraff, B. A. and Demas, J. N. (1994) Direct measurement of rotational correlation times of luminescent ruthenium(II) molecular probes by differential polarized phase fluorometry. *J. Phys. Chem.* **98**, 12478-12480.
2. Lakowicz, J. R., Gryczynski, I., Piszczek, G., Tolosa, L., Nair, R., Johnson, L. M. and Nowaczyk, K. (2000) Microsecond dynamics of biological macromolecules. *Methods Enzymol.* **323**, 473-509.
3. Terpetschnig, E., Szmacinski, H. and Lakowicz, J. R. (1997) Long-lifetime metal-ligand complexes as probes in biophysics and clinical chemistry. *Methods Enzymol.* **278**, 295-321.
4. Haugen, G. R. and Lytle, F. E. (1981) Quantitation of fluorophores in solution by pulsed laser excitation and time-filtered detection. *Anal. Chem.* **53**, 1554-1559.
5. Friedman, A. E., Chambron, J. -C., Sauvage, J. -P., Turro, N. J. and Barton, J. K. (1990) Molecular "light switch" for DNA: $Ru(bpy)_2(dppz)^{2+}$. *J. Am. Chem. Soc.* **112**, 4960-4962.
6. Jenkin, Y., Friedman, A. E., Turro, N. J. and Barton, J. K. (1992) Characterization of dipyridophenazine complexes of ruthenium(II): The light switch effect as a function of nucleic acid sequence and conformation. *Biochemistry* **31**, 10809-10816.
7. Murphy, C. J. and Barton, J. K. (1993) Ruthenium complexes as luminescent reporters of DNA. *Methods Enzymol.* **226**, 576-594.
8. Lakowicz, J. R., Malak, H., Gryczinski, I., Castellano, F. N. and Meyer, G. J. (1995) DNA dynamics observed with long lifetime metal-ligand complexes. *Biospectroscopy* **1**, 163-168.
9. Malak, H., Gryczynski, I., Lakowicz, J. R., Meyers, G. J. and Castellano, F. N. (1997) Long-lifetime metal-ligand complexes as luminescent probes for DNA. *J. Fluorescence* **7**, 107-112.
10. Lakowicz, J. R., Piszczek, G. and Kang, J. S. (2001) On the possibility of long-wavelength long-lifetime high-quantum yield luminophores. *Anal. Biochem.* **288**, 62-75.
11. Lakowicz, J. R. and Maliwal, B. P. (1985) Construction and performance of a variable-frequency phase-modulation fluorometer. *Biophys. Chem.* **21**, 61-78.
12. Feddersen, B. A., Piston, D. W. and Gratton, E. (1989) Digital parallel acquisition in frequency domain fluorimetry. *Rev. Sci. Instrum.* **60**, 2929-2936.
13. Gratton, E., Lakowicz, J. R., Maliwal, B. P., Cherek, H. and Laczko, G. (1984) Resolution of mixtures of fluorophores using variable-frequency phase and modulation data. *Biophys. J.* **46**, 478-486.
14. Lakowicz, J. R., Gratton, E., Laczko, G., Cherek, H. and Limkeman, M. (1984) Analysis of fluorescence decay kinetics from variable-frequency phase shift and modulation data. *Biophys. J.* **46**, 463-477.
15. Patkowski, A., Eimer, W. and Dorfmüller, Th. (1990) Internal dynamics of $tRNA^{phe}$ studied by depolarized dynamic light scattering. *Biopolymers* **30**, 975-983.
16. Jack, A., Ladner, J. E. and Klug, A. (1976) Crystallographic refinement of yeast phenylalanine transfer RNA at 2.5 Å resolution. *J. Mol. Biol.* **108,** 619-649.
17. Robertus, J. D., Ladner, J. E., Finch, J. T., Rhodes, D., Brown, R. S., Clark, B. F. C. and Klug, A. (1974) Structure of yeast phenylalanine tRNA at 3 Å resolution. *Nature* **250**, 546-551.
18. Thomas, J. C., Schurr, J. M. and Hare, D. R. (1984) Rotational dynamics of transfer ribonucleic acid: effect of ionic strength and concentration. *Biochemistry* **23**, 5407-5413.
19. Porschke, D. and Antosiewicz, J. (1990) Permanent dipole moment of tRNA's and variation of their structure in solution. *Biophys. J.* **58**, 403-411.
20. Sipior, J., Carter, J. M., Lakowicz, J. R. and Rao, G. (1996) Single quantum well light-emitting diodes demonstrated as excitation sources for nanosecond phase modulation fluorescence lifetime measurements. *Rev. Sci. Instr.* **67**, 3795-3798.